AUT Journal of Electrical Engineering

AUT J. Elec. Eng., 54(2) (2022) 199-208
DOI: 10.22060/eej.2022.21118.5458

Design of Miniaturized and Biocompatible Antenna with Y-Shaped Slots for Implantable Applications

S. S. Mosavinejad[1], P. Rezaei[2], A. A. Khazaei[1]*

[1] Department of Electrical Engineering, Mashhad Branch, Islamic Azad University, Mashhad, Iran
[2] Electrical and Computer Engineering Faculty, Semnan University, Semnan, Iran

ABSTRACT: A new miniaturized antenna that covers the Industrial Scientific Medical (ISM) band 2.4-2.483.5 GHz is designed. The implantable antenna system consists of a rectangular patch with coaxial feed and Y slots. The compact size of the recommended antenna is 8 × 8 × 1.27 mm^3. A shorting pin is used for miniaturization. In the proposed antenna, the simulated −10 dB bandwidth is about 160 MHz. Enhanced bandwidth (2.39-2.55 GHz) operation can be achieved by introducing ground slots and moving feed and pin to the appropriate position. In a flat type implantable system, the antenna is capsulated with battery and electronic boards. The result was verified by CST software in both heterogeneous multi-layer (skin, fat, and muscle), and homogenous single layer (skin, muscle, stomach, small intestine, and colon) human tissue phantoms. To diagnose the effect of fabrication tolerance and dimensions of slots on impedance and bandwidth, the antenna is parametrically analyzed. For safety consideration and the effects of EM radiation on the human body, the Specific Absorption Rate (SAR) of the antenna is computed. The main features of the designed antenna are the gain value of -15.8 dBi, low SAR, small volume, and large bandwidth that make the proposed antenna an appropriate choice for implantable medical devices. The designed implantable antenna features have been compared with previously reported antennas.

Review History:

Received: Feb. 18, 2022
Revised: Apr. 21, 2022
Accepted: Apr. 23, 2022
Available Online: Dec. 01, 2022

Keywords:

Implantable Antenna
Microstrip Patch Antenna (MPA)
Implantable Medical Devices (IMDs)

1- Introduction

Body-centric Wireless Communications systems (BWCs) like wearable devices, smart implants, and microwave-based sensors have experienced enormous progress over the last decade, and can improve the quality of life and patient's health care and comfort [1-5]. An Antenna plays a significant role as the main part of any wireless IMDs in these devices, and its proper design is one of the challenging issues. The principal aspects that we face in the design of implantable antennas, characterizations, experimental investigations, and guidelines of numerical simulations have been presented in [6-9]. The main parts that we have to deal with in the design of implantable antenna are miniaturization, efficiency, interaction with the human body and biocompatibility, the influence of electronic components, suitable gain, operating frequency and bandwidth, safety, and low SAR considerations [10]. IEEE 802.15.6 supports various frequency bands that are approved for these devices [11]. The Implantable antennas may be fixed inside the human body (e.g., monitoring of diabetes and Increased Intracranial Pressure (ICP), pacemaker), or travel through different human tissues as Wireless Capsule Endoscope (WCE) (e.g., photography, heat therapy and topical radiotherapy).

*Corresponding author's email: khazaei@mshdiau.ac.ir

Recent studies for depth-based and surface-based implant antennas can be categorized and explained in the following. A miniaturized implantable antenna operates dual-band and integrated with the microelectronic components used in scalp implantation and Increased Intracranial Pressure monitoring is presented [12]. In the published article in 2020, a meandered antenna is wrapped inside the endoscopic capsule simulated in a heterogeneous environment and integrated with electronic components with dual-circular polarization, is designed [13]. A research team from Hanyang University, Seoul, has published a spiral-shaped implantable antenna with via-less and a hook-shaped ground slot for scalp implantation and leadless pacemaker systems [14]. Another paper from this team was published in 2018 [15]. In this manuscript, a triple-band implantable small antenna is designed. The antenna integrated system has two architectures, a capsule type and a flat type for deep and surface implantation in the human body. For size reduction and bandwidth enhancement, meandered patch, embedding shorting pin, substrate/superstrate with high permittivity, and open-end slot in the ground plane are used. A miniaturized antenna with slits in the radiating patch and ground surface operating on 915 and 2450 MHz bands with circular-polarization characteristics for WCE application is proposed [16]. A compact volume (9.8) and wide bandwidth antenna with shorting pin and etching open-ended slots in ground plane and patch that operates at 2.45

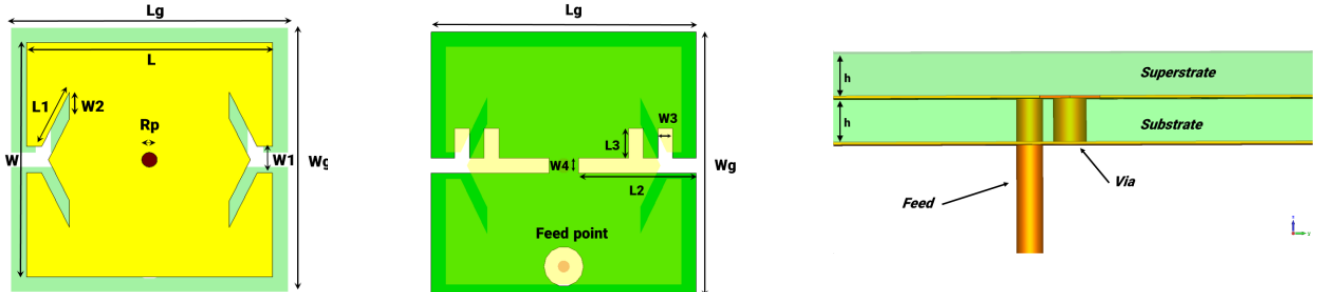

Fig. 1. Structure of the designed antenna (a) Radiating patch (b) Ground plane (c) Side view

GHz is proposed [17]. An E-shaped antenna with meandered arms, operating at 2.4/4.8 GHz used in fully-passive systems and implanted in six subcutaneous locations of a post mortem human body is presented in[18]. To send high-speed signals, an antenna with meandered resonators and Multiple-Input Multiple-Output (MIMO) implantable devices is proposed [19]. Two pairs of triangular and rectangular antennas loaded by a shorting pin and curve slits along lateral sides for retinal prosthesis operating at 1.45 GHz and 2.45 GHz frequencies were introduced [20]. A flower-shape and dual-band (900MHz and 2.4GHz) antenna that included a shorting pin and open-ended slots in the ground plane is introduced [21]. In [22], an antenna is fed by an asymmetric Coplanar Waveguide (CPW) that includes a loop, an asymmetric strip, and a protruding stub with rectangular, U, and L shapes designed for ingestible WCE systems at ISM 2.4GHz band with circular polarization.

A circular patch with a radius of 10 mm, linear polarization, via hole, open-ended slots in the ground surface that operates at the Medical Implant Communication Service (MICS), and 2.4 GHz band is presented in [23]. A pin-loaded annular ring antenna with an L-shaped open-end slot that operates at 2.45GHz is developed[24]. By introducing arc-shaped slots, CP property is achieved. In [25], a circular-implant antenna working at 915 MHz ISM band with wide axial ratio bandwidth has been studied. In another letter [26], a circular and annular-ring circular-shaped antenna operating at 2.4GHz is proposed. A flexible circular ring antenna with an array of metamaterial for gain enhancement and wideband characteristics with CPW-fed in the ISM frequency band is presented [27]. A miniaturized implant antenna, radiating in the ISM band is designed by embedding a Complementary Split-Ring Resonator (CSRR) and C-shaped slots [28].

In this paper, a miniaturized and simple biocompatible antenna at ISM 2.45 GHz band that is suitable for scalp implantation and Wireless Capsule Endoscope systems is introduced. The antenna is designed with an appropriate dimension that has the characteristics of an implantable antenna compared to previous works. In Sect. 2, the design procedure and structure of the antenna are discussed and the performance of the implanted antennas in different tissue models is checked. In Sect. 3, results are presented, and to ensure user safety, SAR is computed.

2- Implantable Antenna Design

In the present study, an implantable patch antenna for biomedical applications is designed to operate in the ISM band, from 2.4 to 2.48 GHz. The human body's lossy behavior, heterogeneous dispersive and anatomical variability between patients alter EM propagation and antenna performance and increase the complexity.

2- 1- Antenna Structure

Fig. 1 shows the geometrical structure of the designed antenna, which has a square-shaped patch and two Y slots. Table 1 shows the detailed parameters of the proposed patch. In our design, Rogers RO6010 (= 10.2, tanδ = 0.0023) with a thickness of 0.635 mm, is used for substrate and superstrate. The antenna is capsulated with 0.1 mm thick biocompatible ceramic alumina (, = 9.8, tan δ = 0.008) to avoid shorting and contact with the surrounding human tissues.

The designed antenna was obtained in four consecutive steps by modifying a basic rectangular patch, as shown in Fig. 2. The conventional patch with 8 × 8 size resonances at 5.15 GHz high frequency (case 1). To shift the operating frequency, two Y slots are embedded. The resonance frequency decreases and shifts from 5.15 GHz to 4.08 GHz, which is still much higher than 2.4 GHz (case 2). Afterwards, a shorting pin with 0.5 mm diameter is created and the resonant frequency decreases to 2.42 GHz (case 3). The proposed patch is fed through a 50-Ω coaxial cable. The distance between the feed point and the center of the patch is 1mm. The simulated bandwidth below −10 dB is from 2.40 GHz to 2.46 GHz. One way to increase bandwidth is to create slots in the ground or patch plane. Enhanced bandwidth (2.39-2.55 GHz) operation can be achieved by introducing ground slots and moving feed and pin at the appropriate position (case 4). By inserting horizontal and vertical slots and optimizing their width and length, we improved the -10dB bandwidth to

Table 1. Detail parameters of the designed patch

Parameters	Value (mm)	Parameters	Value (mm)
Lg	8.5	Rp	0.25
Wg	8.5	L1	0.9
L	8	L2	4
W	8	L3	1
h	0.635	W1	0.9
W2	0.5	W3	0.5
W4	0.5	Ls	2

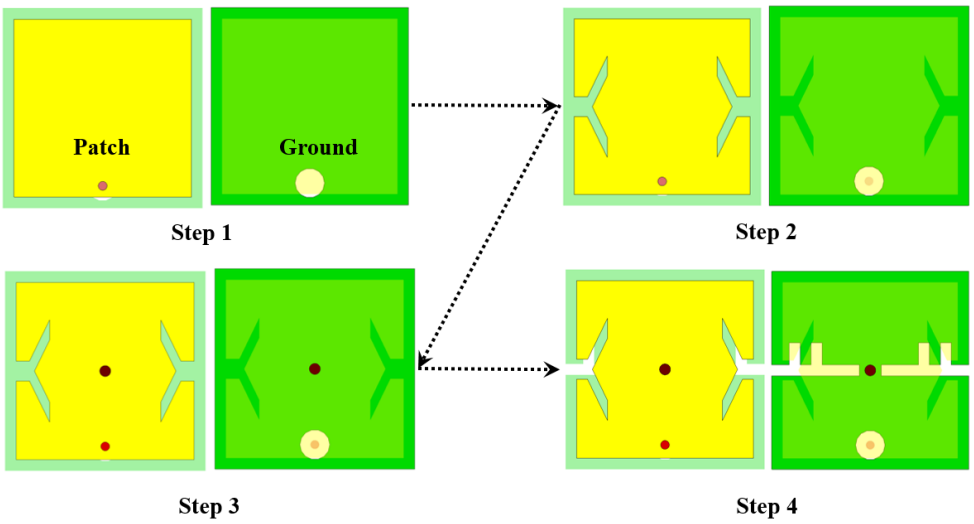

Fig. 2. Design procedure of the implantable antenna with Y-shaped slots

160MHz. Additionally, increasing the height of the substrate and decreasing the height of the superstrate improves the radiation performance of the antenna and gain.

2- 2- Tissue Model

As mentioned earlier, the effect of the human tissue in the analysis and performance evaluation of these antennas must be considered. Thus, an appropriate human tissue model or phantom during the antenna design is crucial for assessment. One-layered cylinder and three-layered phantoms were employed in the past, where dielectric properties for different age groups of both genders are described in [29, 30]. The detail of these models and dielectric properties of human tissue are listed in Table 2 for 2.45 GHz. Furthermore, we consider both homogenous one-layer and tree-layer (skin, fat, and muscle) phantoms to evaluate the antenna in different environments. The dimensions 80 × 80 × 42 and 4mm deep inside of phantom is used to design and simulate the proposed antenna in CST Microwave Studio, as shown in Fig. 3. Changing and increasing the dimensions of the phantom does not affect the resonance frequency and its amount, but the depth of antenna implantation affects the radiating parameters of the antenna. As the implantation depth increases, the antenna gain decreases.

3- Simulation and Results

To predict antenna performance in the presence of humane body, modeling and design procedure were performed with CST simulator using a heterogeneous environment. Due to the near-field strongly coupled with surrounding lossy media, the correct model selection, and assessment is crucial.

3- 1- Reflection Coefficient and Gain Radiation Performance

Fig. 4 shows the reflection coefficient || for different

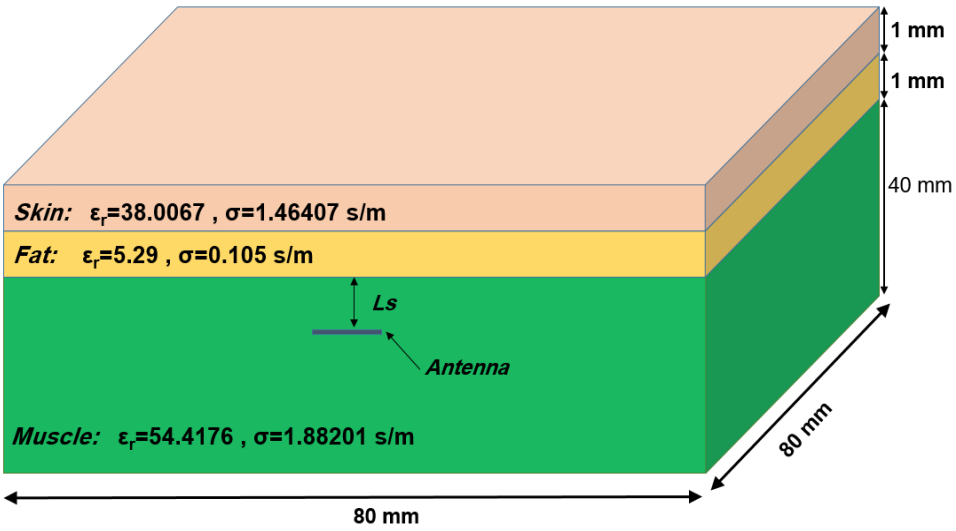

Fig. 3. Heterogeneous phantom in CST

Table 2. Dielectric properties of human tissue at 2.45 GHz [29]

Tissue	ε_r	$\sigma(^{S}/_{m})$	Loss Tangent	Density$(^{kg}/_{m^3})$
Skin	38.1	1.43	0.283	1100
Fat	5.29	0.1	0.145	900
Muscle	52.7	1.74	0.242	1040

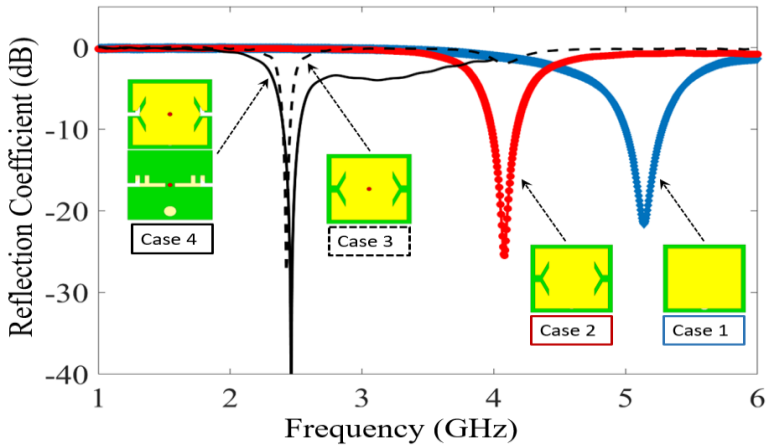

Fig. 4. Reflection coefficient of proposed antenna in multi-layer phantom

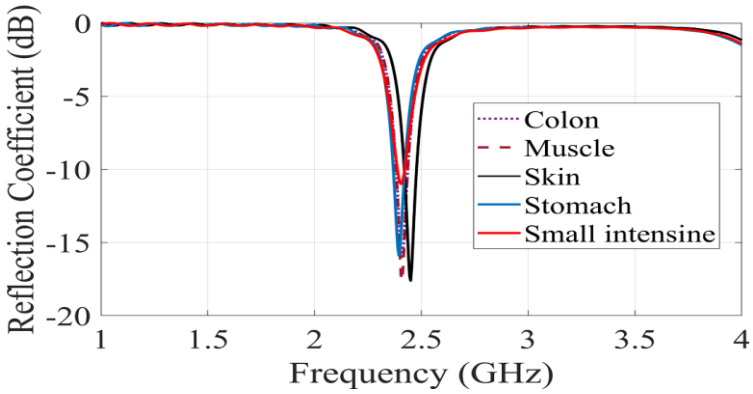

Fig. 5. Reflection coefficient of proposed antenna in single-layer phantoms

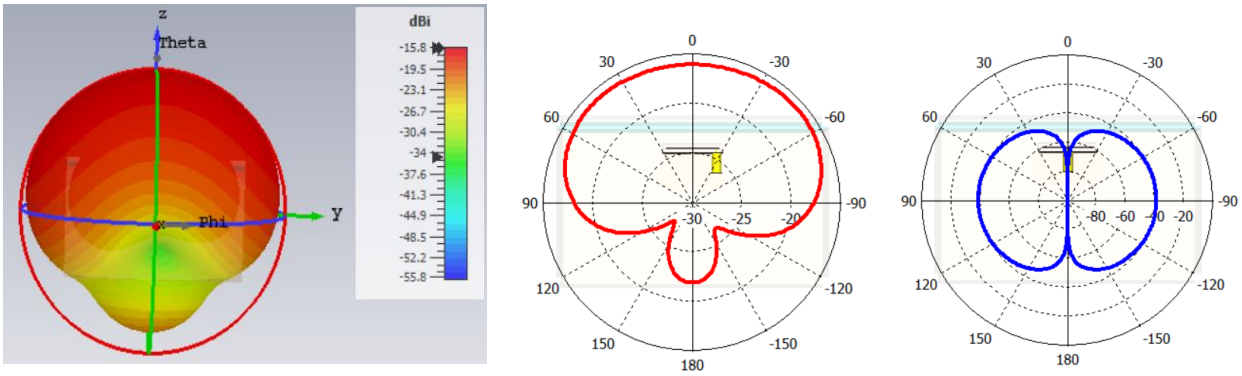

(a) **(b)** **(c)**

Fig. 6. The simulated radiation pattern of the designed antenna at 2.4GHz. (a) 3D radiation pattern. (b) Co-Polarization. (c) Cross- Polarization.

antenna designs, in which the radiating patch, substrate, and superstrate of the antenna have the same size. Fig. 5 shows the return loss for single layer human tissues (skin, muscle, stomach, small intestine, and colon) implementation and this antenna have almost the same function in these tissues and can be used for different applications. The simulated radiation pattern of the designed antenna is presented in Fig. 6, where the maximum gain over the 2.4GHz band is -15.8 dBi.

The current distribution of the designed antenna at resonance frequency is presented in Fig. 7. As demonstrated by Fig. 7, the 2.4 GHz resonance is developed from current flowing to the shorting pin and nearby the Y slots.

3- 2- Implantable System Design and Effects of Electronic Components

For a real device and scenario, antenna should be evaluated in an implantable system. We designed a capsule type with 15×9.2×3.4 dimensions that the proposed antenna is integrated with electronic boards and a battery as shown in Fig. 8. Biocompatible ceramic alumina with 0.1 mm thickness is used for encapsulation. Rogers RO6010 substrate and the Perfect Electric Conductor (PEC) were used for PCB and battery. As shown in Fig. 9 due to the effect of electric components embedded in the implant capsule and Electromagnetic Interference (EMI), the resonance frequency shifted to lower frequencies.

3- 3- Parametric Study

To diagnose the effect of fabrication tolerance and dimensions of slots on impedance and bandwidth, the length and width of the Y-slots (L1, W1), the length and width of the ground slots (L2, L3, W3, W4), and the thickness of the capsule shell were parametrically studied. As L1 and W1 increased, the resonance frequency was shifted but it did not affect antenna bandwidth. By increasing L2 up to 4 mm, the resonance frequency shifts to lower frequencies,

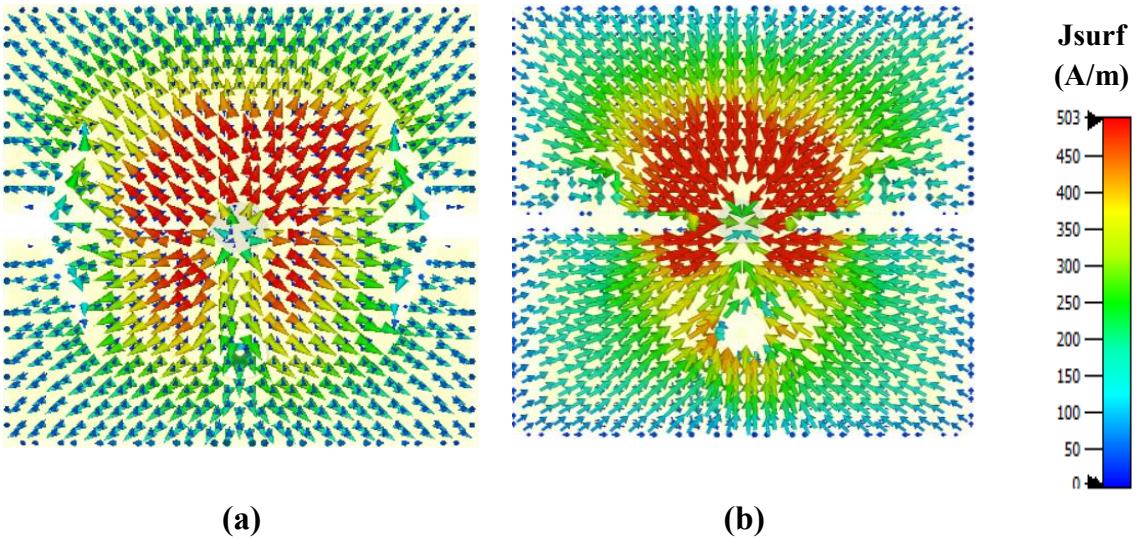

Fig. 7. The current distribution of the designed antenna at 2.45 GHz (a) Radiating patch (b) Ground plane

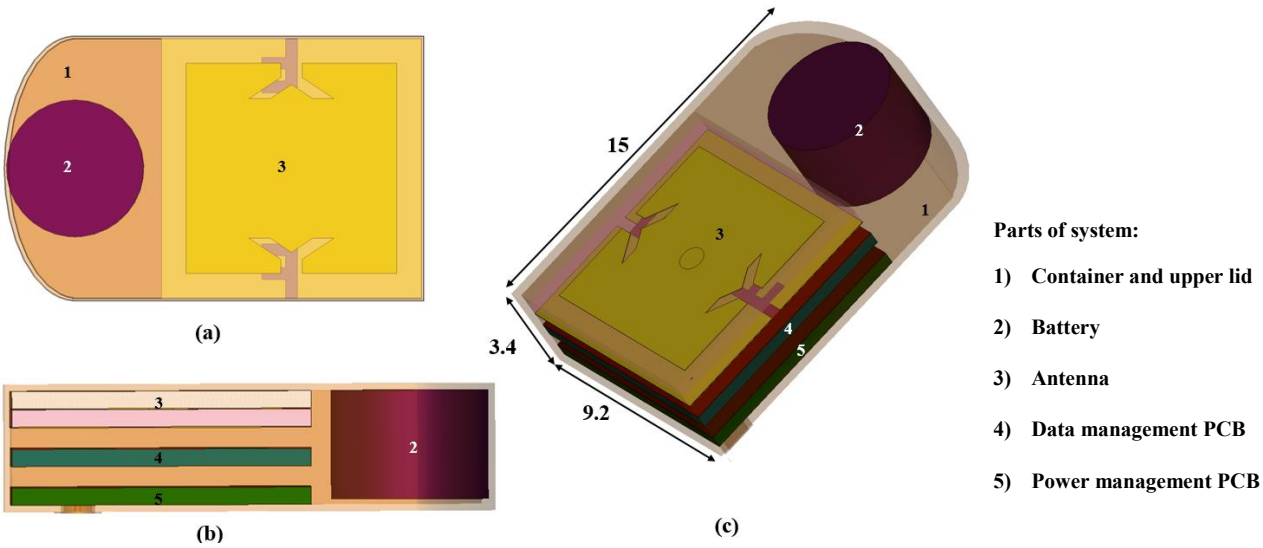

Fig. 8. The implantable device, schematic, and dimensions. (a) Top view. (b) Side view. (c) Isometric view.

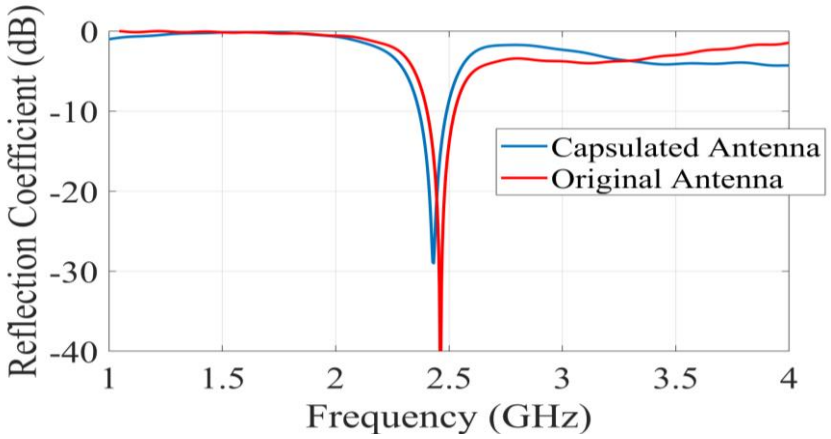

Fig. 9. Coupling effect of the electronic components on the antenna performance

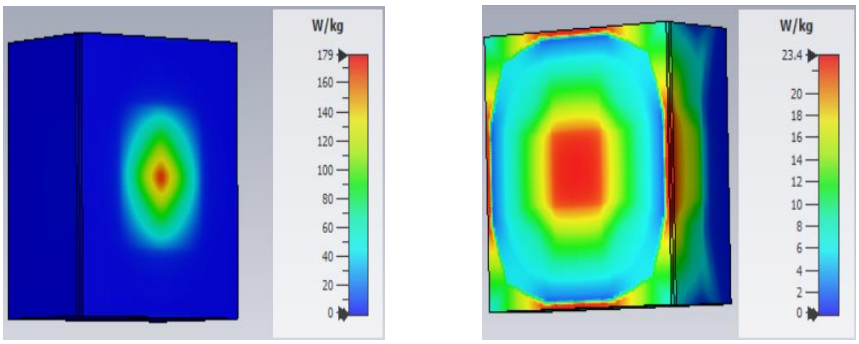

(a) **(b)**

Fig. 10. Simulated SAR level distribution in a three-layer phantom at 2.45 GHz. (a) 1 g of tissue (b) 10 g of tissue.

and the bandwidth of the antenna increases. By increasing W4 up to 0.5 mm, the resonance frequency is shifted to higher frequencies. The thickness of the capsule shell affects the radiation parameters of the implantable antenna. By thickness increasing, it observed that the resonance frequency moves upward. According to these parametric studies, the optimal values given in Table 1, were selected for antenna characteristics and the encapsulation thickness was set to 0.1 mm.

3- 4- SAR Consideration

For safety consideration and effects of antenna radiation on the human body, by simulating the three-layered phantom in CST, the SAR value of the antenna has been computed. Maximum acceptable values for SAR measurement are established by several regulations. IEEE C95.1-1999 specifies a maximum SAR of 1.6 W/kg in a cube of 1 g of tissue and C95.1-2005 regulation establishes a limit of 2 W/kg over a 10 g of tissue [31]. The SAR value for 1g and 10g of tissue is confirmed to be 179 W/kg and 23.4 W/kg, respectively, as shown in Fig. 10. Therefore, to satisfy the SAR requirement, the maximum input power applied to the designed antenna is limited to 8.9 mW.

Finally, the characteristic and radiation features of the designed antenna have been compared with previously reported manuscripts in Table 3 [32-35]. It is observed that the proposed implant antenna has competencies and biocompatibility features such as low SAR, small size, large bandwidth, and high gain compared to other reported antennas.

Table 3. Comparison of the designed antenna with other works

Ref.	Year	Freq. (GHz)	Dimension (mm^3)	Dielectric material (ε_r)	Patch Shape	Pin	SAR1g, max [W/kg]	G_{max} [dBi]	-10dB-BW [MHz]	Polar.
[12]	2018	0.9 2.45	8×6×0.5	Rogers6010 (10.2)	Rec.	No	971 807	-28.5 -22.8	90 210	LP LP
[14]	2019	0.4 1.6 2.45	7×6.5×0.377	Rogers 6010 (10.2)	Rec.	No	588 441 305	-30.5 -22.6 -18.2	148 171 219	LP LP LP
[15]	2018	0.9 1.9 2.45	7×6×0.5	Rogers 6010 (10.2)	PIFA	Yes	363 358 380	-20.4 -23 -26.4	79 155 178	LP LP LP
[16]	2020	0.9 2.45	6.5×6.5×0.5	Ultralam 3850HT(2.9)	Rec	No	420 233	-28.2 -24.5	124.7 152.8	CP CP
[17]	2021	2.45	7×7×0.2	Rogers Ultralam(2.9)	Rec.	Yes	350.8	-15.8	1533	LP
[18]	2018	2.4 4.8	7.7×6.9×1.52	TMM 13i (12.85)	Rec.	Yes	337 571.5	-16.7 -12	80 115	LP/LP
[20]	2020	2.45	7×6.93×1.27	Rogers 6010 (10.2)	Trian.	Yes	111	-	900	LP
[21]	2018	0.9 2.45	7×7.2×0.2	Rogers Ultralam(2.9)	Rec.	Yes	471 313	-28.4 -26.6	184 219.7	LP LP
[22]	2018	2.45	16.6×14.2×0.254	Rogers 6010 (10.2)	Rec.	Yes	368.7	-29.1	780	CP
[23]	2018	0.4 2.4	$\pi \times 10^2 \times 2.54$	Rogers 6010 (10.2)	Circular	Yes	241.5 149.5	-34 -15.2	152 420	LP
[26]	2017	2.45	$\pi \times 5.5^2 \times 1.27$	Rogers 3010 (10.2)	Circular	No	733.5	-22.7	199	CP
[28]	2016	2.45	8.5×8.5×1.27	Rogers 3210 (10.2)	CSRR	Yes	210.8	-17	293	CP
[32]	2016	0.4 2.45	22×23×1.27	Rogers3010 (10.2)	Rec.	Yes	832 690	-36.7 -27.1	30 168	LP LP
[33]	2017	2.45	10×10×1.27	Rogers 6010 (10.2)	Truncated Rec.	Yes	-	-27.2	150	CP
[34]	2018	2.45	16×16×0.275	Silicon (11.7)	CSRR	No	269	-16.5	2150	LP
[35]	2019	2.45	$\pi \times 5^2 \times 0.5$	RF-35 (3.5)	Circular	No	568.2	-20.75	330	LP
This work	-	2.45	8×8×1.27	Rogers6010 (10.2)	Rec.	Yes	179	-15.8	160	LP

4- Conclusion

A new miniaturized antenna that covers the ISM band (2.4-2.483.5 GHz) is designed. By embedding Y slots on the radiator and a shorting pin, miniaturization was achieved, and by creating slots on the ground plane and moving feed and pin at the appropriate position and adjusting the width of slots, enhanced bandwidth operation can be achieved. The result was verified by CST software in a three-layer phantom. Antenna performance in single-layer human tissues (skin, muscle, stomach, small intestine, and colon) has also been investigated. For safety consideration, SAR value of the antenna has been computed. The antenna is integrated with Perfect Electric Conductor s and a battery and the effects of electronic components are analyzed. Finally, the designed MPA features are compared with previously antennas proposed in recent years.

References

[1] W. Greatbatch, C.F. Holmes, History of implantable devices, IEEE Eng Med Biol Mag, 10(3) (1991) 38-41.

[2] S. Kiani, P. Rezaei, M. Fakhr, A CPW-fed wearable antenna at ISM band for biomedical and WBAN applications, Wireless Networks, 27(1) (2021) 735-745.

[3] A. Zarkhoshk, P. Rezaei, A Compact Wearable Antenna for UWB and Bluetooth Applications, Tabriz Journal of Electrical Engineering, 48(2) (2018) 679-686.

[4] M. Najjariani, P. Rezaei, Three-Band, Flexible, Wearable Antenna with Circular Polarization, in: Fundamental Research in Electrical Engineering, Springer, 2019, pp. 987-996.

[5] E. Atashpanjeh, P. Rezaei, Broadband conformal monopole antenna loaded with meandered arms for wireless capsule endoscopy, Wireless Personal Communications, 110(4) (2020) 1679-1691.

[6] J. Kim, Y. Rahmat-Samii, Implanted antennas inside a human body: Simulations, designs, and characterizations, IEEE Transactions on microwave theory and techniques, 52(8) (2004) 1934-1943.

[7] A. Kiourti, K.S. Nikita, A review of implantable patch antennas for biomedical telemetry: Challenges and solutions [wireless corner], IEEE Antennas and Propagation Magazine, 54(3) (2012) 210-228.

[8] A. Kiourti, K.S. Nikita, Recent advances in implantable antennas for medical telemetry [education column], IEEE Antennas and Propagation Magazine, 54(6) (2012) 190-199.

[9] A. Kiourti, K.S. Nikita, A review of in-body biotelemetry devices: Implantables, ingestibles, and injectables, IEEE Transactions on Biomedical Engineering, 64(7) (2017) 1422-1430.

[10] A. Kiourti, K.S. Nikita, Implantable Antennas: A Tutorial on Design, Fabrication, and In Vitro\/In Vivo Testing, IEEE Microwave Magazine, 15(4) (2014) 77-91.

[11] S.A. Salehi, M.A. Razzaque, I. Tomeo-Reyes, N. Hussain, IEEE 802.15. 6 standard in wireless body area networks from a healthcare point of view, in: 2016 22nd Asia-Pacific Conference on Communications (APCC), IEEE, 2016, pp. 523-528.

[12] S.A.A. Shah, H. Yoo, Scalp-implantable antenna systems for Increased Intracranial Pressure monitoring, IEEE Transactions on Antennas and Propagation, 66(4) (2018) 2170-2173.

[13] A. Basir, M. Zada, Y. Cho, H. Yoo, A dual-circular-polarized endoscopic antenna with wideband characteristics and wireless biotelemetric link characterization, IEEE Transactions on Antennas and Propagation, 68(10) (2020) 6953-6963.

[14] I.A. Shah, M. Zada, H. Yoo, Design and analysis of a compact-sized multiband spiral-shaped implantable antenna for scalp implantable and leadless pacemaker systems, IEEE Transactions on Antennas and Propagation, 67(6) (2019) 4230-4234.

[15] M. Zada, H. Yoo, A miniaturized triple-band implantable antenna system for bio-telemetry applications, IEEE Transactions on Antennas and Propagation, 66(12) (2018) 7378-7382.

[16] S. Hayat, S.A.A. Shah, H. Yoo, Miniaturized dual-band circularly polarized implantable antenna for capsule endoscopic system, IEEE Transactions on Antennas and Propagation, 69(4) (2020) 1885-1895.

[17] M. Yousaf, I.B. Mabrouk, M. Zada, A. Akram, Y. Amin, M. Nedil, H. Yoo, An ultra-miniaturized antenna with ultra-wide bandwidth characteristics for medical implant systems, IEEE Access, 9 (2021) 40086-40097.

[18] J. Blauert, Y.-S. Kang, A. Kiourti, In vivo testing of a miniature 2.4/4.8 GHz implantable antenna in postmortem human subject, IEEE Antennas and Wireless Propagation Letters, 17(12) (2018) 2334-2338.

[19] A.J. Alazemi, A. Iqbal, A High Data Rate Implantable MIMO Antenna for Deep Implanted Biomedical Devices, IEEE Transactions on Antennas and Propagation, (2021).

[20] S. Bahrami, G. Moloudian, S.R. Miri-Rostami, T. Björninen, Compact Microstrip Antennas With Enhanced Bandwidth for the Implanted and External Subsystems of a Wireless Retinal Prosthesi, IEEE Transactions on Antennas and Propagation, 69(5) (2020) 2969-2974.

[21] F. Faisal, H. Yoo, A miniaturized novel-shape dual-band antenna for implantable applications, IEEE Transactions on Antennas and Propagation, 67(2) (2018) 774-783.

[22] R. Li, Y.-X. Guo, G. Du, A conformal circularly polarized antenna for Wireless Capsule Endoscope systems, IEEE Transactions on Antennas and Propagation, 66(4) (2018) 2119-2124.

[23] N. Ganeshwaran, J.K. Jeyaprakash, M.G.N. Alsath, V. Sathyanarayanan, Design of a dual-band circular implantable antenna for biomedical applications, IEEE Antennas and Wireless Propagation Letters, 19(1) (2019) 119-123.

[24] L.-J. Xu, Y. Bo, W.-J. Lu, L. Zhu, C.-F. Guo, Circularly polarized annular ring antenna with wide axial-ratio bandwidth for biomedical applications, IEEE Access, 7 (2019) 59999-60009.

[25] Y. Zhang, C. Liu, X. Liu, K. Zhang, X. Yang, A wideband circularly polarized implantable antenna for 915 MHz ISM-band biotelemetry devices, IEEE Antennas and Wireless Propagation Letters, 17(8) (2018) 1473-1477.

[26] R. Li, Y.-X. Guo, B. Zhang, G. Du, A miniaturized

circularly polarized implantable annular-ring antenna, IEEE Antennas and Wireless Propagation Letters, 16 (2017) 2566-2569.

[27] S. Das, D. Mitra, A compact wideband flexible implantable slot antenna design with enhanced gain, IEEE Transactions on Antennas and Propagation, 66(8) (2018) 4309-4314.

[28] X.Y. Liu, Z.T. Wu, Y. Fan, E.M. Tentzeris, A miniaturized CSRR loaded wide-beamwidth circularly polarized implantable antenna for subcutaneous real-time glucose monitoring, IEEE Antennas and Wireless Propagation Letters, 16 (2016) 577-580.

[29] S. Gabriel, R.W. Lau, C. Gabriel, The dielectric properties of biological tissues: III. Parametric models for the dielectric spectrum of tissues, Phys Med Biol, 41(11) (1996) 2271-2293.

[30] C. Gabriel, Dielectric properties of biological tissue: variation with age, Bioelectromagnetics, 26(S7) (2005) S12-S18.

[31] W.H. Bailey, R. Bodemann, J. Bushberg, C.-K. Chou, R. Cleveland, A. Faraone, K.R. Foster, K.E. Gettman, K. Graf, T. Harrington, Synopsis of IEEE Std C95. 1™-2019 "IEEE Standard for Safety Levels With Respect to Human Exposure to Electric, Magnetic, and Electromagnetic Fields, 0 Hz to 300 GHz", IEEE Access, 7 (2019) 171346-171356.

[32] Y. Liu, Y. Chen, H. Lin, F.H. Juwono, A novel differentially fed compact dual-band implantable antenna for biotelemetry applications, IEEE Antennas and Wireless Propagation Letters, 15 (2016) 1791-1794.

[33] Z.-J. Yang, S.-Q. Xiao, L. Zhu, B.-Z. Wang, H.-L. Tu, A circularly polarized implantable antenna for 2.4-GHz ISM band biomedical applications, IEEE Antennas and Wireless Propagation Letters, 16 (2017) 2554-2557.

[34] S. Bhattacharjee, S. Maity, S.R. Bhadra Chaudhuri, M. Mitra, Metamaterial-inspired wideband biocompatible antenna for implantable applications, IET Microwaves, Antennas & Propagation, 12(11) (2018) 1799-1805.

[35] S. Hout, J.-Y. Chung, Design and characterization of a miniaturized implantable antenna in a seven-layer brain phantom, IEEE Access, 7 (2019) 162062-162069.

HOW TO CITE THIS ARTICLE

S. S. Mosavinejad, P. Rezaei, A. A. Khazaei, Design of Miniaturized and Biocompatible Antenna with Y-Shaped Slots for Implantable Applications, AUT J. Elec. Eng., 54(2) (2022) 199-208.

DOI: 10.22060/eej.2022.21118.5458